Water Air Soil Pollut (2021) 232: 176
https://doi.org/10.1007/s11270-021-05105-3

In Situ Evaluation of Filter Media Modified by Biocidal Nanomaterials to Control Bioaerosols in Internal Environments

Paula de Freitas Rosa Remiro · Cristina Paiva de Sousa · Henrique Cezar Alves · André Bernardo · Mônica Lopes Aguiar

Received: 23 November 2020 / Accepted: 31 March 2021 / Published online: 19 April 2021

Abstract Controlling the bioaerosol present in indoor environments has been evidenced to be extremely necessary. An alternative is to develop filter media for air conditioners that have biocidal properties. This study aimed to verify the biocidal effect of a high-efficiency particulate air (HEPA) filter medium modified with the deposition of nanoparticles on its surface. For this purpose, Ag, TiO_2, and Ag/TiO_2 nanoparticles were used and the antimicrobial activities of these nanomaterials against *Escherichia coli*, *Staphylococcus aureus*, and *Candida albicans* microorganisms were evaluated, as well as the biocidal efficacy of the modified HEPA filter with these nanomaterials in a real environment. The percentages of elimination obtained for the Ag, TiO_2, and Ag/TiO_2 nanomaterials, respectively, were 53%, 63%, and 68% (*E. coli*); 67%, 67%, and 69% (*S. aureus*); and 68%, 73%, and 75% (*C. albicans*). The HEPA filter media had their surfaces modified by aspersion and deposition of Ag, TiO_2, and Ag/TiO_2 nanomaterials. We could conclude that the nanoparticles adhered to the filter medium do not affect its permeability. The modified filters were arranged in an internal environment (bathroom) for the collection of the bioaerosols, and after the collection, the filter cake was plated and arranged to grow in a liquid medium. The results showed that the filters have 100% of biocidal action in passing air, and 55.6%, 72.2%, and 81% of inhibition to microbial growth in their surface for modification with Ag, TiO_2, and Ag/TiO_2, respectively, compared to unmodified filters.

Keywords Biocidal nanomaterials · Indoor pollution · Bioaerosol · Air filtration

Highlights
•Synthesis and characterization of silver nanoparticles (AgNPs), titania nanoparticles (TiO_2NPs), and a titania-silver nanocomposite;
•Evaluation of the biocidal capacity of the nanomaterials against Gram-negative bacteria, Gram-positive bacteria, and fungi;
•Modification of HEPA filter by deposition of nanomaterials with biocidal characteristics, without significant change on filter permeability;
•Evaluation of the biocidal capacity of the filters modified with nanomaterials in a realistic application in which filters were exposed to a real heterogeneous population of microorganisms;
•Comparison between the performance of the nanomaterial against specific microorganisms and the modified filter against a realistic exposure to bioaerosol.

P. de Freitas Rosa Remiro · A. Bernardo (✉) · M. L. Aguiar
Chemical Engineering Department, Federal University of São Carlos, São Carlos, SP, Brazil
e-mail: abernardo@ufscar.br

C. P. de Sousa · H. C. Alves
Morphology and Pathology Department, Federal University of São Carlos, São Carlos, SP, Brazil

1 Introduction

Research concerning nanomaterials has increased rapidly in recent years, largely due to their advantageous characteristics relative to the corresponding bulk materials, including enhanced surface area and high reactivity. Nanomaterials such as silver and titanium dioxide have been widely reported in the literature because of their great antimicrobial activities (Kim et al., 2009).

The techniques used to synthesize silver nanoparticles include green synthesis routes (biosynthesis) employing fruit (Kumar et al., 2017), plants (Amooaghaie et al., 2015; Raja et al., 2017), algae (Palanisamy et al., 2017), and microalgae extracts (Ferreira et al., 2017) as reducing agents. Silver nanoparticles can also be synthesized using microemulsion (Krutyakov et al., 2008; Zhang et al., 2007), electrochemical (Ma et al., 2004), microwave-assisted (Eustis Krylova et al., 2005), and chemical reduction methods (Gorup et al., 2011; Lee & Meisel, 1982; Pillai & Kamat, 2004), among others. In this work, an established chemical reaction method was used for the synthesis, because it was essential to ensure that the tests performed were repeatable and reproducible. Biological matrices differ considerably, which could lead to non-reproducible results. The selected reaction was the reduction of silver nitrate using sodium citrate as a reducing agent.

Titanium dioxide nanoparticles can also be produced by green methods using plant (Sivaranjani & Philominathan, 2016; Suman et al., 2015) and fungal (Durairaj et al., 2014) extracts, as well as by microwave (Estruga et al., 2010), sonochemical (Hassanjani-Roshana et al., 2011), and sol-gel procedures. The sol-gel technique is widely used to synthesize titanium nanoparticles and was chosen here due to its simplicity and reproducibility (Lazarevic et al., 2010; Malekfar et al., 2009; Šalkus et al., 2012).

Silver nanoparticles exhibit excellent antifungal activity against *Trichosporon asahii* (Xia et al., 2016) and *Candida* spp. (Panacek et al., 2009) and can inhibit bacteria such as *Brucella melitensis* (Alizadeh et al., 2013) and *Pseudomonas chlororaphis* (Calder et al., 2012). Titanium dioxide nanoparticles exert inhibitory effects against the bacteria *Pseudomonas putida* (Combarros et al., 2016) and the fungi *Hypocrea lixii* (white-rot) and *Mucor circinelloides* (brown-rot) (Filpo et al., 2013). These materials, when bound, can give rise to materials called composites. A silver and titanium dioxide nanocomposite has been tested as an antimicrobial agent (Cao et al., 2011). Research concerning the use of nanomaterials as antibiotics has increased due to the problem of resistance of pathogens to antibiotics (Conlon et al., 2004).

Many regions worldwide are affected by worsening air quality, with over 80% of urban populations in cities where the pollution levels are higher than those recommended by the World Health Organization limits. These levels can cause health impacts, including a greater risk of strokes, heart disease, lung cancer, and chronic and acute respiratory diseases such as asthma (WHO, 2017). The many atmospheric pollutants include bioaerosols consisting of viruses, bacteria, and fungi (Ross et al., 2000). Air quality problems occur in indoor environments where the accumulation of microorganisms is associated with poor air exchange, and increases in asthma attacks and bronchial hyperreactivity have been linked to increased bioaerosol levels (Ross et al., 2000). The COVID-19 pandemic has exacerbated the already existing indoor pollution problem and its consequences.

Filters can be used to remove particulate material from the air in indoor environments, although the collected bioaerosols may still include live organisms. Therefore, it is necessary to develop methodologies and materials (antimicrobials) that are capable of inhibiting these microorganisms. Considering the possible application of nanomaterials to control microorganisms present in the air, it is necessary to evaluate the potential of such materials to eliminate or inhibit the microorganisms commonly found in internal environments. Many methodologies can be used to evaluate the antimicrobial power of nanomaterials. The diffusion method is widely employed, where the degree of halo inhibition indicates the effectiveness of the studied material (Ahmad et al., 2013; Arshi et al., 2011; Freitas et al., 2014; Ninan et al., 2014; Prema et al., 2017; Ravichandran et al., 2016; Tian et al., 2016; Turki et al., 2012). Another way of evaluating the antimicrobial effect of materials is to measure the optical density based on the MacFarland scale. This scale enables the calculation of the number of cells in a sample (Selvamani et al., 2016). In this study, both of these methodologies were used, since only one of the nanomaterials could be evaluated using the disk diffusion method. Three different microorganisms (one Gram-positive bacterium, one Gram-negative bacterium, and one fungus) were used in the elimination/inhibition tests. Evaluation of the effectiveness of the materials studied was the essential first step in the development of products to be used in real environments. However, to the authors' knowledge, there is only a previous study of our group in the literature that tests filtration media in a real environment (Rosa et al., 2017). Usually, in the literature, several studies aim to evaluate the action of antimicrobials with a single microorganism, or a few microorganisms, while a test in a real environment can evaluate the action of antimicrobials in a wide range of microorganisms acting

simultaneously. That is why the efficacy of filter media modified by those nanomaterials to mitigate microbial contamination in a real air filtration condition was also tested.

Thus, this work aimed to evaluate the power of the elimination of microorganisms by different biocidal nanomaterials, as well as the capability of a filter medium modified with those materials to mitigate bioaerosol contamination during a real application.

2 Materials and Methods

2.1 Synthesis and Characterization of the Nanomaterials

Silver nanoparticles were synthesized according to the method of Turkevich et al. (Turkevich et al., 1951), with the formation of metallic silver by the reduction reaction between silver nitrate (Synth) and sodium citrate (Synth, 99%). TiO_2 nanoparticles were synthesized by the method proposed by Pechini (Pechini, 1967), with the reaction between citric acid (Q_{hemis}, 99.5–100.5%) and titanium isopropoxide (Sigma-Aldrich, 97%) generating titanium citrate, which is a high-viscosity polymer precursor. This precursor was calcined at 400 °C for 60 min for removal of the organic material and formation of the oxide of interest. The Ag/TiO_2 nanocomposite was initially synthesized by the method proposed by Pan (Pan et al., 2010). However, the nanocomposites produced by this method did not show crystallinity, so the synthesis route was modified with the incorporation of a calcination step (900 °C for 120 min), which resulted in the formation of crystalline nanocomposites.

The structure, composition, and particle size distribution (PSD) of the synthesized materials were characterized using scanning electron microscopy (SEM), X-ray diffractometry (XRD), and dynamic light scattering (DLS). The SEM analyses were performed using Philips XL-30 FEG SEM (field emission gun) and FEI Magellan 400 L instruments, both coupled to an energy-dispersive detector (EDS). The XRD analyses were performed using a Siemens D5005 instrument, and the PSD determination was based on DLS measurements employed a Malvern Zetasizer Nano ZS90 system. For the PSD measurements, the TiO_2 nanoparticles and the Ag/TiO_2 nanocomposites were suspended in a 2.5 wt% aqueous solution of sodium dodecyl sulfate (Sigma-Aldrich, 99.0%).

2.2 Antibacterial Activity

Deliberate contamination was performed using the Gram-negative bacterium *Escherichia coli* (ATCC 11775), the Gram-positive bacterium *Staphylococcus aureus* (ATCC 29213), and the yeast *Candida albicans*. These microorganisms were chosen because they represented different types of pathogens and are commonly found in many environments.

Antimicrobial susceptibility was evaluated using the agar disk diffusion method. The colonies were suspended in sterile saline (0.85%) until turbidity corresponding to 10^7 CFU/mL on the MacFarland scale was reached. Aliquots (10 μL) of the suspensions were then added to Petri dishes containing the Mueller-Hinton agar medium and distributed over the entire surface with the aid of a Drigalski strap (spread plate method). Paper filter disks (6 mm diameter) were then placed on the surface of the inoculated medium, with light pressure from a flanged clamp to ensure adherence to the culture medium. After this procedure, 5- and 10-μL aliquots of the antimicrobial agent solution (6 μg/L) were added to the side disks of the plate and 10 μL of water (as a control) was added to the central disk. The plates were then incubated in a laboratory oven at 37 °C for 24 h. The diameters (in mm) of the inhibition halos around each disk were measured with the aid of a pachymeter. This procedure followed the methodology proposed by Bauer et al. (Bauer et al., 1966).

The optical density method was used to estimate the percentage of inhibition of microbial growth. Aliquots of 9.95 mL of 1% sulfuric acid (Sigma-Aldrich, 99.99%) and 0.05 mL of 1.175% barium chloride (Sigma-Aldrich, 99%) were added to a 10-mL tube. This solution had a concentration of 1.5×10^8 g/mL, corresponding to 0.5 on the MacFarland scale. The solution was stored at room temperature, protected from light. The resuspended barium sulfate precipitate corresponded to the density obtained for a culture of microorganisms in a liquid medium at a concentration of 1.5×10^8 CFU/mL. A calibration curve was then constructed using optical density measurements performed with a Biospectro SP-22 spectrophotometer. For this, tubes were prepared with 15 mL of Mueller-Hinton culture medium, to which 10^3 cells/mL of the microorganisms, 2.5 mg of the nanomaterial to be studied, and 1% (v/v) of dispersing agent (Tween 80) were added. The tubes were incubated at 37 °C for 24 h, followed by measurement of optical density. For calculation of the

final values, the absorbance of positive control solution (containing the microorganisms and Tween 80, without the nanomaterial) was subtracted from the total absorbance.

2.3 Aerosol Generation and Modification of Filter Media

The fiberglass high-efficiency particulate air (HEPA) filters were modified through the aerosol generation of the three different nanomaterials (silver, titanium, and titania silver composite) over 2 h with 0.17 g/L concentration suspensions and velocity of 5 cm/s through the aerosol generation of nanomaterials. The system used was already explained in detail elsewhere as in the work of Rosa et al. (Rosa et al., 2018). It consists of (1) air purification filters, (2) aerosol generator, (3) diffusion dryer, (4) radioactive Kr-85 neutralizer, (5) filter medium support, (6) manometer, (7) radioactive Am-241 neutralizer, (8) flowmeter, and (9) electrostatic classifier, condensation particle counter, and computer for data acquisition.

2.4 Measurement of Permeability of the Filter Media, Before and After Surface Modification

The permeability was obtained through the velocity drop pressure curves generated in the equipment detailed by Rosa et al. (Rosa et al., 2018).

For the pressure drop measurements, initially, the media was cut into the appropriate size (124.6 mm in diameter) to be allocated to the support. Subsequently, with the aid of the rotor, the flow of fluid through the filter medium was varied. For each velocity variation, a value for the pressure drop was recorded and subsequently used in the permeability calculation. The calculation was performed using the Darcy equation (1).

The Darcy equation was chosen for use because the experiment was performed at low speeds.

$$\frac{\Delta P}{L} = \frac{\mu}{k_1} \cdot \upsilon_s \tag{1}$$

where k_1 corresponds to Darcy's permeability (also known as viscous permeability), ΔP is the pressure drop, L is the thickness of the filter medium, μ is the viscosity of the air, and υ_s is the superficial velocity.

2.5 In Situ Collection of Particulate Matter

To collect the bioaerosols and to determine the number of microorganisms to be sampled, the filtration system presented in Fig. 1 was used, which consisted of three rotary flowmeters: brand Nalgene, model 315-0047; ASA, 400 to 1600 L/h, and a model 820 vacuum pump of the Fisatom brand. The system was specially constructed for this purpose, based on Catranis et al. (Catranis et al., 2006). The experimental apparatus was placed in the selected room (bathroom) where air filtration was performed using a filtration system of Fig. 1. The system was composed of two funnels, each of these funnels being used to simultaneously expose the modified filter (with the nanoparticles) and the unmodified filter, to obtain a comparison under the same sampled conditions: brand Nalgene, model 315-0047; three ASA rotary flowmeters, 400 to 1600 L/h; and a Fisatom brand model 820 vacuum pump as shown in Fig. 1. The hopper funnel is attached to a stem whose height to the ground is adjustable, and in this research, the height of 1.50 m was used (RE/ANVISA n° 9, of January 16, 2003). The system consisted of the modified filter and a series of HEPA to evaluate the elimination/inhibition of the retained bioaerosol and through air (see Fig. 1). The collections were done in triplicate for each of the three modifications (with the three different nanomaterials), but only one comparative measure was made at a time; each pair of triplicate was probably exposed to different populations of microorganisms.

2.6 Evaluation of the Percentage of Inhibition/ Elimination of Bioaerosols

The inhibition of microorganisms found in the real environment was evaluated qualitatively by plating the material in Petri dishes and quantitatively by assessment of the dry mass content of microorganisms.

2.6.1 Plating (Qualitative Method)

The Nutrient Agar-type culture medium of 5 g/L compositions of peptone and sodium chloride, 1.5 g/L of meat extract and yeast extract, and 1.5 g/L of agar (Merck brand, Mikrobiologie series) was used for culture bacteria and fungi and prepared according to the recommendations indicated on the label, which corresponds to a quantity of 20 g of the product for each liter of distilled water. Soon after this medium was stored in

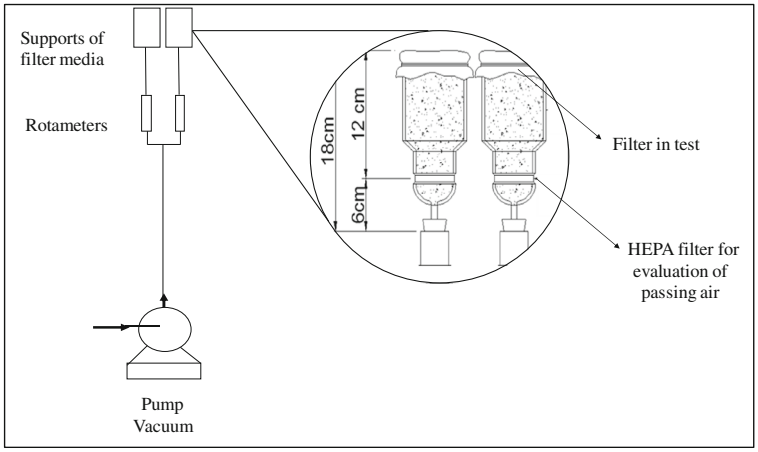

Fig. 1 Equipment used to collect the particulate matter

appropriate flasks and sterilized in a vertical autoclave at 120 °C for 15 min to ensure that no microorganisms were present in it, the medium was stored in the refrigerator. To use the medium, it was heated in a microwave oven and about 10 mL of the medium was applied to each sterilized Petri dish.

A volume of 50 mL of 0.9% NaCl solution (sodium chloride) was used to wash the filters. This solution was stirred to ensure that all particulate materials were suspended in the solution. Then, a volume of 0.5 mL was transferred to the Petri dish, and with the help of a Drigalski loop, this volume was spread across the plate. The cultivation of the microorganisms was done in a shaker, which allows the control of temperature and agitation which were 37 °C and 120 rpm. After preliminary tests, it was noted that the best incubation time was 48 h.

2.6.2 Dry Mass Method—Quantitative Method

The methodology chosen to quantitatively evaluate the content of microorganisms was dry mass (Tortora et al., 2006). In this method, the Falcon tubes (polypropylene tubes) were initially placed in greenhouses at 60 °C to eliminate all the moisture present in it. They were then placed in desiccators to maintain the low humidity. Subsequently, the tubes were weighed, and the values were taken note of. Cultures were performed like that previously described and after 48 h, 10 mL of the culture medium containing the cells was extracted and placed in Falcon tubes for further centrifugation. After centrifugation, the supernatant was discarded and the tubes containing the cells were brought to the oven at 60 °C. After 18 h in the oven, the tubes were withdrawn and returned to desiccators until reaching room temperature. Finally, the tubes were weighed. Calculation of the dry mass was performed by subtracting the mass of the tube from the mass of the tube containing the cells. This procedure was done for both filters (modified with nanomaterials and unmodified).

For calculation of the inhibition/elimination content, a calculation was made considering the dry mass obtained in the unmodified filter as 100%, and the dry mass of the modified filter was weighted. Thus, by comparing the contents obtained in the two filters, the inhibition/elimination content was assigned the difference between the values found between the modified and the non-modified filters, since the filters were arranged in the internal environment at the same time and under the same conditions.

3 Results and Discussion

3.1 Synthesis and Characterization of the Nanomaterials

The synthesized nanoparticles were characterized by SEM, XRD, and DLS. Figure 2, 3, and 5 show SEM images and EDS spectra of the silver nanoparticles, of the surface composition of the TiO_2, and the Ag/TiO_2 nanoparticles, respectively.

It can be seen from Fig. 2a that the particles were nano-sized. The particle size was subsequently confirmed by PSD measurements. The peaks obtained were in the same region (at approximately 3 keV) as the peaks reported by Hebeish et al. (Hebeish et al., 2013). The other two materials, being solid, were confirmed by the X-ray diffraction technique.

The TiO_2 nanoparticle agglomerates are shown in Fig. 3a. Costa et al. (Syafiuddin et al., 2017) reported that these agglomerates have characteristics of soft agglomerates (formed by van der Waals forces) since they could be easily disintegrated using a mortar and 200-mesh sieves. The determination of PSD using DLS confirmed that the primary TiO_2 particles were nanosized. Figure 3b shows the presence of titanium and oxygen peaks in the EDS spectrum, hence confirming the presence of TiO_2.

XRD measurements were performed to determine the crystalline structure of the TiO_2 particles. The resulting X-ray diffractogram is shown in Fig. 4.

Comparison of the diffractogram for the synthesized sample with the Crystallographica Search-Match database, considering the diffraction planes, interplanar distances, and atomic/electron densities, indicated that the synthesized solid corresponded to titanium dioxide nanoparticles with rutile structure.

The Ag/TiO_2 nanocomposite agglomerates are shown in Fig. 5a, from which it can be seen that the agglomerates were nanostructured, consisting of primary nanoparticles. Figure 5b shows the EDS spectrum used to confirm the composition of the synthesized solid. The presence of silver, titanium, and oxygen indicated the existence of Ag/TiO_2 nanocomposite, as subsequently confirmed using the XRD technique (Fig. 6).

The X-ray diffractogram for the Ag/TiO_2 solid (Fig. 6) showed that the material was crystalline, with peaks corresponding to rutile-phase titanium dioxide (shown in red) and silver (shown in blue). The presence of distinct peaks for the two species was indicative of the presence of the materials, silver, and titanium grains and characteristic of a composite. The most intense 2θ peaks for the synthesized sample corresponded to the most intense peaks in the standard TiO_2 and Ag diffractograms. The small differences in the peak intensities could have been due to the ways that the samples were prepared.

The results of the PSD measurements based on the DLS technique of the nanomaterials are shown in Fig. 7. The polydisperse distribution obtained for the silver nanoparticles (Fig. 7a) showed four modes, reflecting a mixture of four particle populations with mean sizes of around 2 nm, 7 nm, 50 nm, and 300 nm. The largest mode was indicative of the presence of agglomerates (even in aqueous suspension) since the SEM analysis showed a typical size of 30–50 nm. The mean size for the entire distribution was 39 nm.

The TiO_2 particles showed a monodisperse distribution (Fig. 7b), with particles varying in size from 300 to 700 nm, in agreement with the SEM analysis. Therefore, regardless of whether the synthesis route produced primary particles of smaller size, the image analysis and DLS measurements indicated the existence of a population with a larger mean size, even in aqueous suspension. The mean size determined by DLS was 421 nm.

The results for the Ag/TiO_2 nanocomposites (Fig. 7c) clearly showed two particle populations, one with a mean size of around 160 nm and the other with a mean size of around 500 nm. The mean size of the entire distribution was 368 nm. The DLS results indicated that the agglomerates broke down in the aqueous dispersion, as shown in the image analysis (Fig. 7a).

3.2 Antibacterial Activity

After synthesis and characterization of the nanomaterials, an evaluation was made of their antimicrobial effects. Figures 8, 9, and 10 illustrate disks treated with the suspension of silver nanoparticles applied to the plates containing *E. coli*, *S. aureus*, and *C. albicans*. The images denoted by (a) and (b) are duplicates. In total, four disks were used for each volume of nanomaterial (5 μL and 10 μL), and two central disks were used as controls (treatment with water alone).

The images shown in Figs. 8, 9, and 10 revealed the formation of inhibition halos (clear zones around the antimicrobial disks) due to diffusion of the antimicrobial agent from the filter paper disks through the solid medium, hence inhibiting microbial growth. The diameters of the inhibition halos (in mm) were 9 ± 1.4 (5 μL) and 10.5 ± 0.58 (10 μL) for *E. coli*, 7.8 ± 0.5 (5 μL) and 11.5 ± 2.4 (10 μL) for *S. aureus*, and 8.0 ± 0.0 (5 μL) and 10.8 ± 0.5 (10 μL) for *C. albicans*. The data of the inhibition halos are in agreement with the data presented in the literature. Syafiuddin et al. (Nurul Aini et al., 2019) obtained inhibition data of 7.7 mm and 10 mm for *Bacillus cereus* and *E. coli*, respectively, using silver nanoparticles produced with the natural oxidizing agent *Carica papaya*. However, using the agents *Manihot esculenta* and *Morinda citrifolia*, no inhibition halo was observed (Nurul Aini et al., 2019). Aini et al. (Nurul Aini et al., 2019) studied the antibacterial capacity of silver nanoparticles produced by the extracts of *Talinum triangulare*, *Ageratum conyzoides*, and

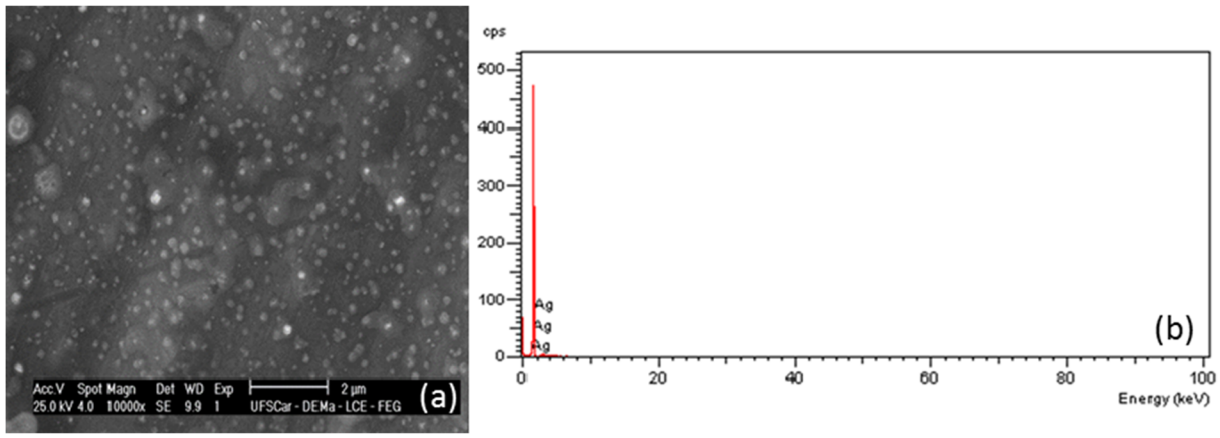

Fig. 2 **a** SEM image and **b** EDS analysis of the surface composition of the silver nanoparticles

Mikania micrantha and obtained values of inhibition halo for the microorganism *E. coli* of 2.35 ± 0.35, 1.27 ± 0.06, and 1.3 ± 0.5, respectively. The nanoparticles produced with *Talinum triangulare* extract was also tested for the microorganisms *S. aureus* and *C. albicans*, and inhibition halo values of 2.55 ± 0.64 and 1.65 ± 0.07 were obtained (Syafiuddin et al., 2018).

The same group of authors of the two previously mentioned studies investigated the antimicrobial power of silver produced with extracts of *Cyperus rotundus*, *Eleusine indica*, *Euphorbia hirta*, *Melastoma malabathricum*, *Clidemia hirta*, and *Pachyrhizus erosus*. The inhibition halos obtained for the bacterium *E. coli* were 15.00 ± 0.36, 12.30 ± 0.06, 12.30 ± 0.50, 1.60 ± 0.10, 1.60 ± 0.10, and 11.00 ± 0.05, respectively (Costa et al., 2006). Thus, as reported in these data found in the literature, it is noted that the silver nanoparticles produced in this work have a close and sometimes higher inhibitory power than those found in the literature.

The disk diffusion test only revealed inhibition in the case of the silver nanomaterial (Figs. 8, 9, and 10). The TiO_2 and Ag/TiO_2 nanomaterials showed no inhibition (no halo formation), which could have been due to poor diffusion of these materials in the agar. According to the Einstein-Stokes equation ($D = \kappa_B T / 6\pi\eta r$), diffusivity is inversely proportional to the radius of the particle. Therefore, since the radii of the titanium dioxide and nanocomposite particles were approximately 10 times larger than the radius of the silver particles, their diffusivities were 10 times lower, hence explaining the formation of an inhibition halo only in the case of the silver nanoparticles. Another possible reason for the absence of a halo was poor dispersion of the nanomaterials, which tended to settle in the bottom of the bottles, hindering pipetting and homogenization. SDS could

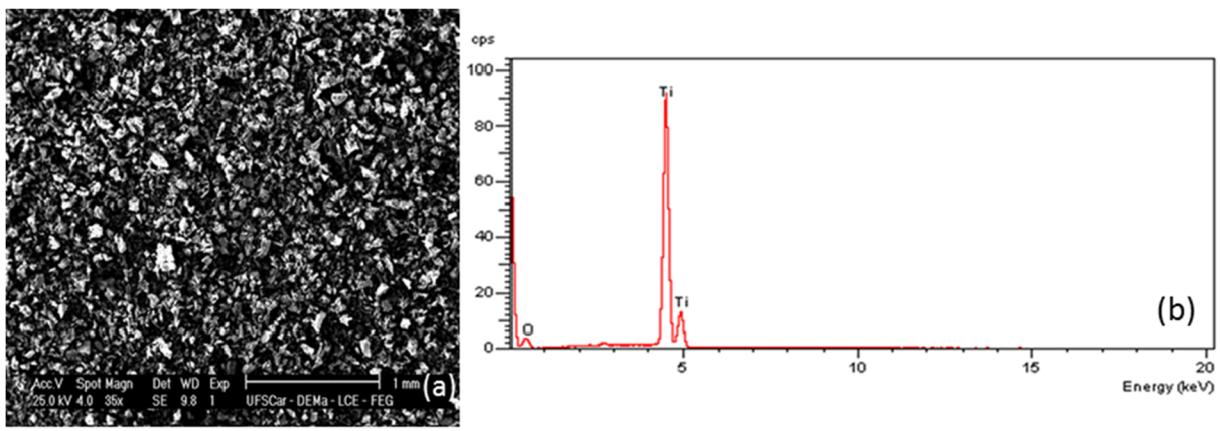

Fig. 3 **a** SEM image and **b** EDS analysis of the surface composition of the TiO_2 nanoparticles.

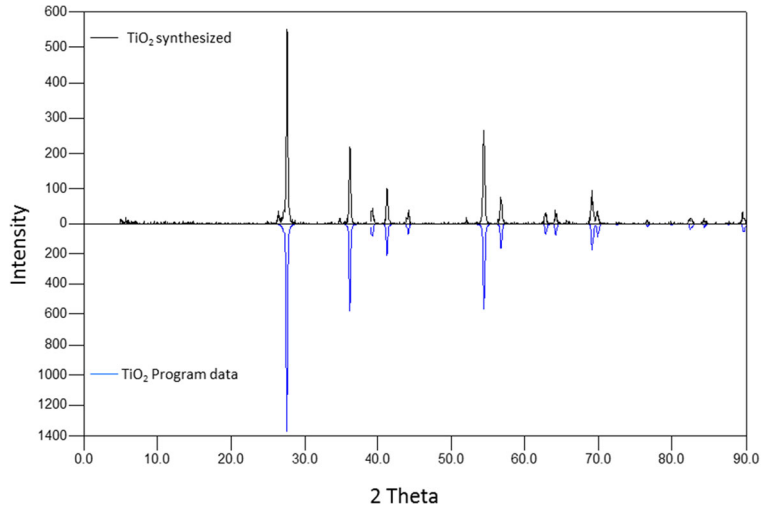

Fig. 4 X-ray diffractogram of the TiO_2 nanomaterial

not be used in this test, because its inherent antimicrobial activity would have biased the results. Therefore, a 1% (v/v) concentration of Tween 80 was used; although this was probably insufficient to satisfactorily suspend the particles, a higher concentration of Tween 80 would also have shown antimicrobial activity.

After completion of the disk diffusion assays and confirming that only the silver nanoparticles caused inhibition halos, the optical density tests were performed. The results are shown in Tables 1, 2, and 3.

The elimination percentages obtained for the Ag, TiO_2, and Ag/TiO_2 nanomaterials, respectively, were 53%, 63%, and 68% (*E. coli*); 67%, 67%, and 69% (*S. aureus*); and 68%, 73%, and 75% (*C. albicans*). According to Allaker (Allaker, 2010), the antimicrobial properties of synthetic or natural materials such as TiO_2, ZnO, fullerene, chitosan, carbon nanotubes, and silver nanoparticles can be due to several different mechanisms (Tortora et al., 2006). The photocatalytic production of reactive oxygen species can destroy cell components of the microorganisms (as in the case of TiO_2) or disrupt the cell membrane and electron transport (as in the case of silver nanoparticles). Figure 11 illustrates some of the mechanisms that can trigger cell death and, consequently, the death of microorganisms. It can be seen from Tables 1, 2, and 3 that the highest inhibition percentages were obtained using the Ag/TiO_2 nanocomposite. The data suggested that the greater effect of the hybrid material was due to a combination of the mechanisms mentioned above. The mechanisms of action of silver and titanium are different, so their combined effects made the nanomaterial more effective, with evidence of synergism (the combined effect was greater than the sum of the individual effects of the agents).

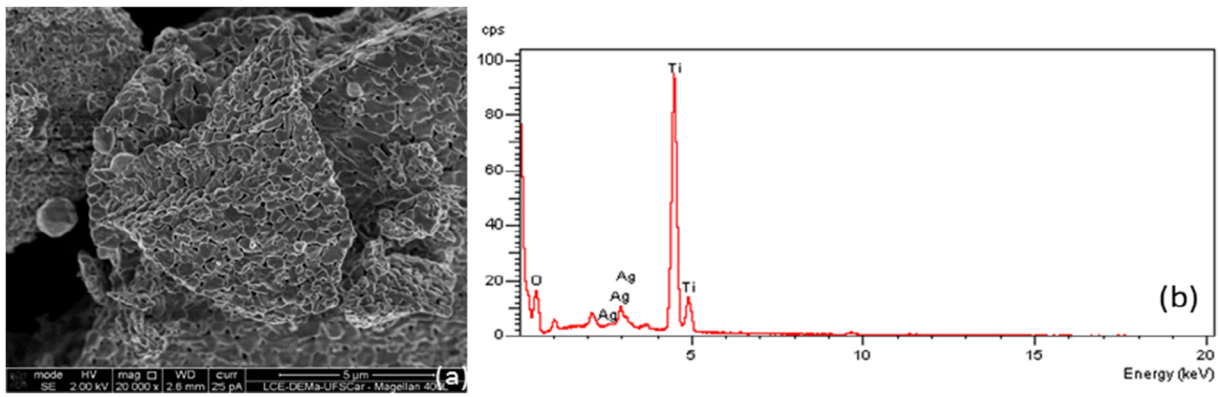

Fig. 5 **a** SEM image and **b** EDS analysis of the surface composition of the Ag/TiO_2 nanocomposite

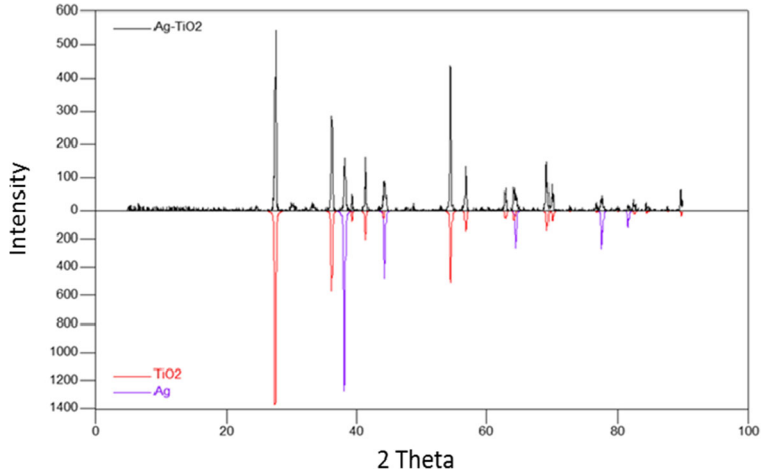

Fig. 6 X-ray diffractogram of the Ag/TiO_2 nanocomposite

The differences among the reduction percentages observed for the three microorganisms could have been due to the differences in anatomy and physiology. It is also possible that there were different probabilities of an encounter between the microorganisms and the particles since it is likely that not all the microorganisms were exposed to the nanomaterials, leading to divergences in the inhibition percentages. However, the same mass of nanomaterial was utilized in all the experiments, and the larger surface area/volume ratio for the silver nanoparticles meant that many more particles were present in the experiments employing silver, which would be expected to increase the probability of collisions between the microorganisms and the particles. Considering these effects, it seems that the differences in elimination percentages could be best explained by the different anatomical and physiological characteristics of the three microorganisms.

3.3 Aerosol Generation and Modification of Filter Media and Evaluation of Permeability

After evaluating the biocidal potential of the materials, a change of the surface (deposition of nanoparticles) of the filter media was performed.

To evaluate if the materials present in the fibers caused an increase in pressure drop, and consequent energy expenditure in its application, permeability measurements of the filtering medium before and after the modification were made.

Figure 12 shows the pressure drop per length ($\Delta P/L$) × surface velocity of the unmodified filter and the modified filter media by each of the three nanomaterials.

With the angular coefficient of this curve, it is possible to obtain the permeability value of the filter media. It is possible to notice a similarity between the curves, and after calculations, it is concluded

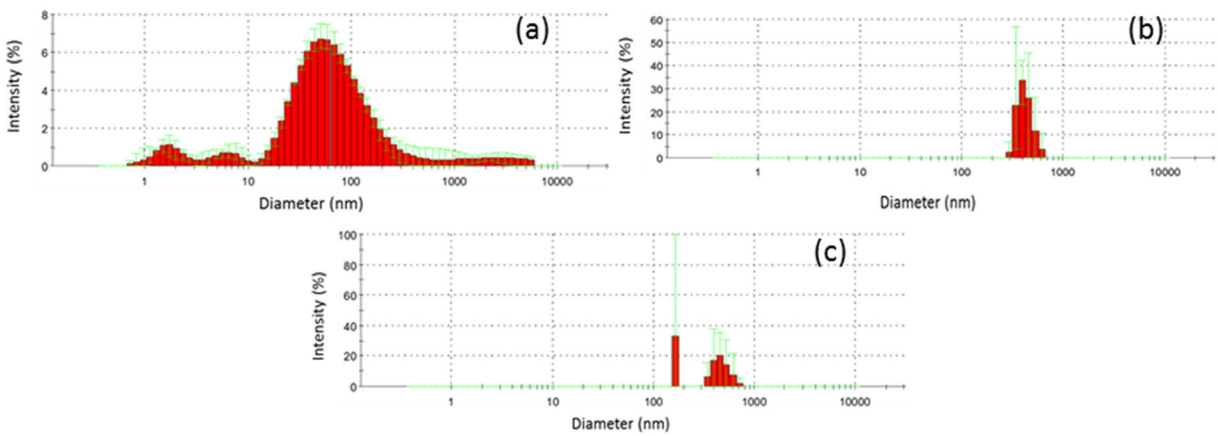

Fig. 7 Particle size distributions of the nanomaterials. **a** Silver. **b** TiO_2. **c** Ag/TiO_2

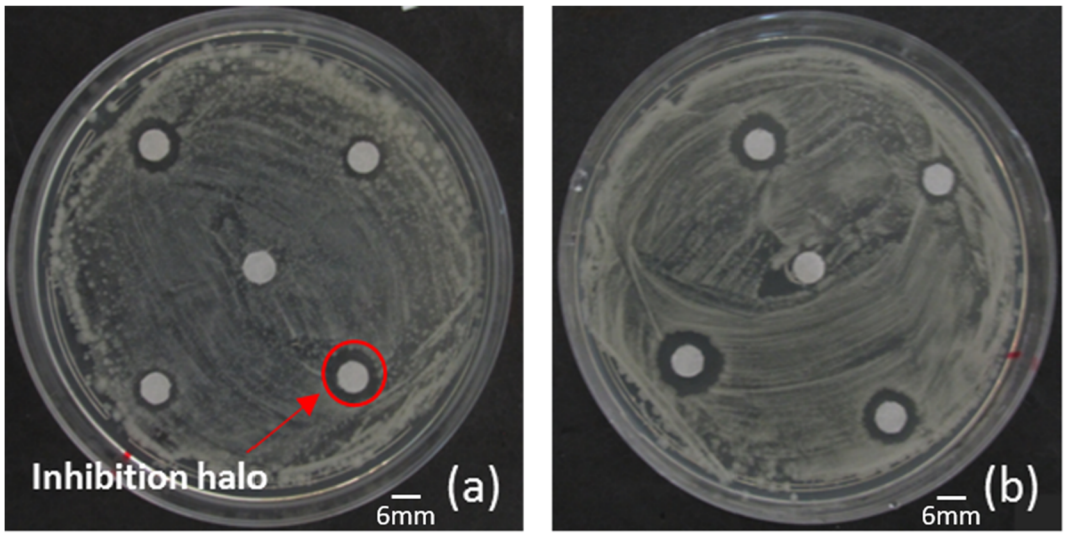

Fig. 8 a, b Agar disk diffusion assay for *E. coli* with silver nanoparticles

that the permeabilities of the four filters used ((1) filter in the absence of modification, (2) filter with silver nanoparticles, (3) filter with titanium dioxide nanoparticles, and (4) filter with nanocomposite titania silver) were between 1.79×10^{-12} and 1.84×10^{-12} m^2, reiterating the idea that the modifications on the surface do not alter the permeability value of the filter media. Thus, the use of materials on the surface of the medium filter does not require additional energy to operate the device in which the filter will be allocated (such as air conditioning, for example).

3.4 In Situ Collection of Particulate Matter and Evaluation of the Percentage of Inhibition/Elimination of Bioaerosols

After modifying the filter media with the nanomaterials and evaluating that the particles do not affect the pressure drop, the filter media were subjected to particulate material collection followed by plating of this collected material.

Images of the Petri dishes containing the inoculums of the modified and unmodified Ag filters after 48 h of incubation are shown in Fig. 13.

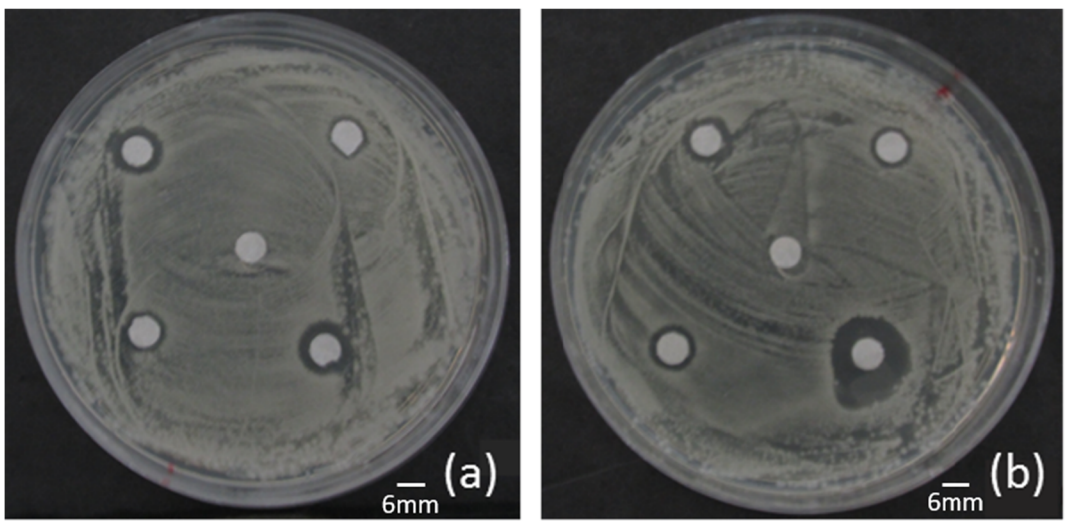

Fig. 9 a, b Agar disk diffusion assay for *S. aureus* with silver nanoparticles

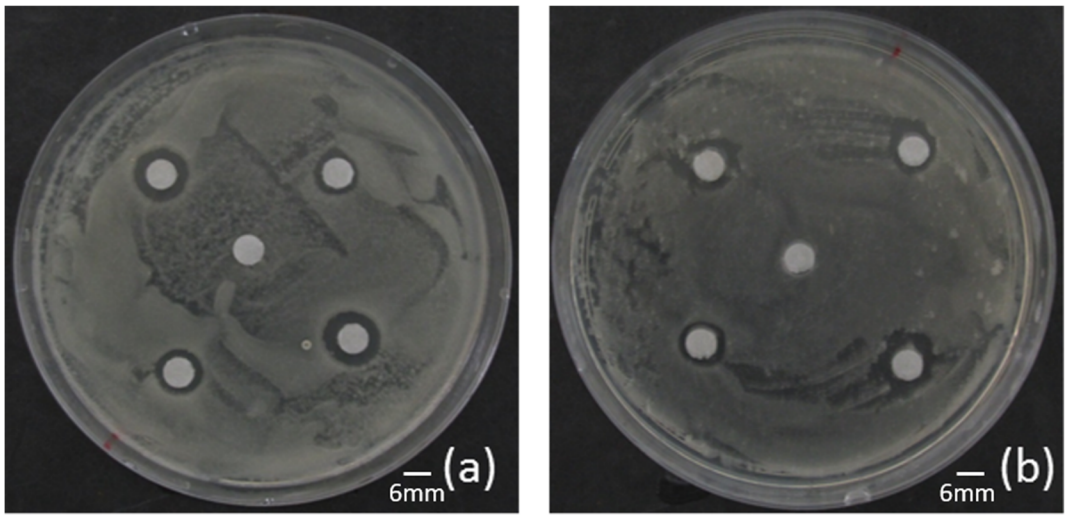

Fig. 10 a, b Agar disk diffusion assay for *C. albicans* with silver nanoparticles

These images were obtained to perform the counts of CFUs present in each of the tests. However, due to the presence of filamentous microorganisms and the difficult counting of the number of microorganisms, the images were used to illustrate qualitatively what was found quantitatively.

The qualitative tests were done in triplicate to find out if they had the same behavior. From Fig. 13, it can be seen that the Petri dish of the modified filters (Fig. 13a) and the plates of the unmodified filters (Fig. 13b) did not show significant differences in terms of the difference of microorganism colonies.

Figure 13 suggests a decrease in retained contamination (passing air has no contamination in all conditions), but it was impossible to quantify such a decrease, so the dry mass method was used to quantitatively determine the inhibition efficiency. This test was also run in triplicate so that the standard deviation of the samples could be calculated. Table 4 presents the dry mass values obtained from the culture of microorganisms contained in the particulate material in filters unmodified and modified with silver nanomaterials. It can be seen that the inhibition in all three tests was greater than 50%. The mean inhibition was 55.6 ± 9.52%, showing that silver has an antimicrobial effect not very pronounced but enough to halve the microorganisms in an environment.

Images of the Petri dishes containing the inoculums of modified and non-modified TiO_2 filters after 48 h of incubation are shown in Fig. 14.

From Fig. 14, it can be seen that the Petri dish of the modified filters (Fig. 14a) has a much smaller number of colonies as compared to the plates of the unmodified filters (Fig. 14b). This result qualitatively demonstrates the efficiency of inhibition of the microorganisms in filter media containing TiO_2.

To evaluate quantitatively, the dry mass method was also implemented. Table 5 presents the dry mass values obtained from the culture of microorganisms contained

Table 1 Average absorbance data obtained in the optical density test (*E. coli*)

Nanomaterial	Average absorbance	Cells number (comparison with McFarland solution)	Elimination percentage (%)
TiO_2	0.262 ± 0.009	3.35E+07	62.942 ± 1.257
Ag/TiO_2	0.241 ± 0.002	3.08E+07	65.959 ± 0.294
Blank (TiO_2 and Ag/TiO_2 measurements)	0.707 ± 0.031	9.04E+07	0.000
Control	0.584 ± 0.004	7.47E+07	17.397
Ag	0.209 ± 0.010	2.67E+07	53.144 ± 2.204
Blank (Ag measurements)	0.445 ± 0.029	5.69E+07	0.000

Table 2 Average absorbance data obtained in the optical density test (*S. aureus*)

Nanomaterial	Average absorbance	Cells number (comparison with McFarland solution)	Elimination percentage (%)
TiO_2	0.100 ± 0.006	1.27E+07	66.741 ± 1.555
Ag/TiO_2	0.092 ± 0.006	1.17E+07	69.410 ± 1.897
Blank (TiO_2 and Ag/TiO_2 measurements)	0.300 ± 0.005	3.83E+07	0.000
Control	0.284 ± 0.012	3.63E+07	5.228
Ag	0.082 ± 0.027	7.35E+06	67.474 ± 10.18
Blank (Ag measurements)	0.276 ± 0.013	2.26E+07	0.000

in the particulate material in filters unmodified and modified with TiO_2 nanomaterials.

It can be seen that inhibition in all three tests was greater than 66%. The mean inhibition was 72.2 ± 4.81%, showing that titanium dioxide has a greater antimicrobial effect than silver since it is possible to observe the variety of microorganisms found in the collection environment. According to Rajagopal et al. (Rajagopal et al., 2006), this inhibition is probably due to the formation of H_2O_2 which is quite toxic to the cell wall, thus causing the death of microorganisms.

Images of Petri dishes containing the inoculums of modified and unmodified Ag/TiO_2 filters after 48 h of incubation are shown in Fig. 15.

From Fig. 15, it can be seen that the Petri dish of the modified filters (Fig. 15a) has a much smaller number of colonies as compared to the plates of the unmodified filters (Fig. 15b) or to Ag and TiO_2 isolate. Note that in two of the three trials, no microorganisms appeared on the modified filter plate. The qualitative assay demonstrates that the composite was more efficient than Ag and TiO_2 alone, suggesting that there is a synergistic effect. To evaluate quantitatively, the dry mass method was also implemented. Table 6 shows the dry mass values obtained from the culture of microorganisms contained in the particulate material in the filters unmodified and modified with Ag/TiO_2 nanomaterials.

It can be seen that the inhibition in all three tests was greater than 80%. The mean inhibition was 81.11 ± 1.92%, showing that the Ag/TiO_2 nanocomposite is the nanomaterial that has the best antimicrobial effect in real environments.

Table 7 summarizes the mean data obtained from the evaluation of modified filter media in real environments.

The data suggested that the greatest effect of the hybrid material was due to a combination of the mechanisms of microorganism inhibition of silver and titanium dioxide. According to Le Ouay and Stellacci (2015), nanoparticles can bring significant improvements in antibacterial activity through specific effects, such as adsorption on bacterial surfaces. However, the mechanism of action is essentially driven by the oxidative dissolution of the nanoparticles. The role of Ag^+ release in the mechanism of action has also been addressed in numerous studies and explains the sensitivity of the antimicrobial activity to the presence of some chemical species, mainly halides and sulfides that form insoluble salts with Ag^+. Foster et al. (Foster et al., 2011) in their work gave an overview of the effects of photoactivated TiO_2 on microorganisms. The activity was shown to be

Table 3 Average absorbance data obtained in the optical density test (*C. albicans*)

Nanomaterial	Average absorbance	Cells number (comparison with McFarland solution)	Elimination percentage (%)
TiO_2	0.114 ± 0.009	1.46E+07	72.842 ± 2.075
Ag/TiO_2	0.104 ± 0.006	1.33E+07	75.218 ± 1.432
Blank (TiO_2 and Ag/TiO_2 measurements)	0.421 ± 0.020	5.38E+07	0.000
Control	0.405 ± 0.030	5.05E+07	3.800
Ag	0.143 ± 0.006	1.82E+07	67.892 ± 1.280
Blank (Ag measurements)	0.444 ± 0.023	5.68E+07	0.000

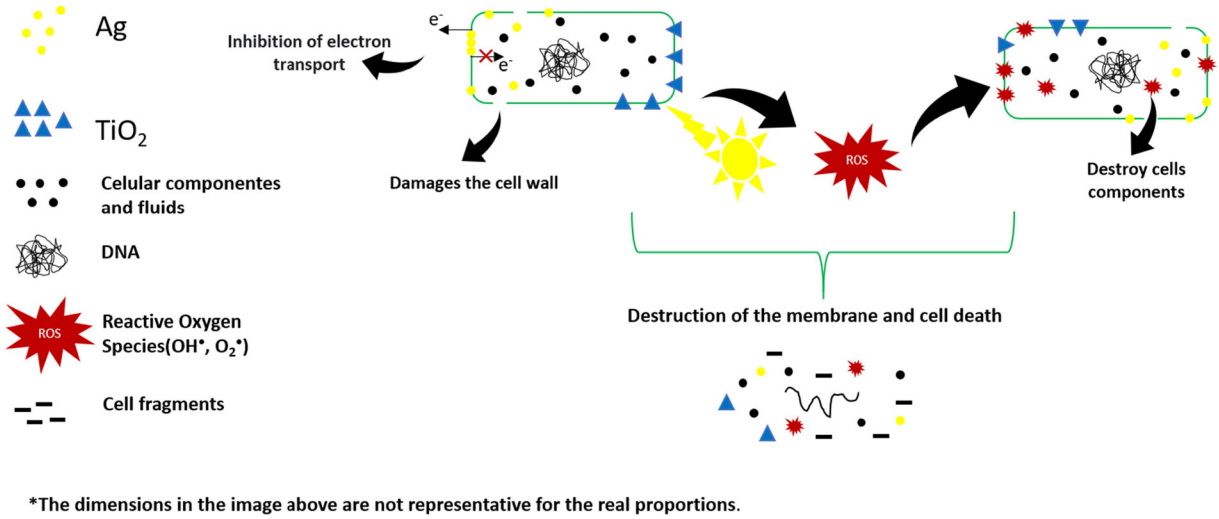

Fig. 11 Schematic diagram of toxicity of Ag and TiO_2 nanoparticles to microorganisms

able to exterminate a wide range of Gram-negative and Gram-positive bacteria and filamentous and unicellular fungi, among others. The mechanism of death involves the degradation of the cell wall and cytoplasmic membrane due to the production of reactive oxygen species, such as hydroxyl radicals and hydrogen peroxide. This initially leads to leakage of cellular content, then cell lysis, and can be followed by complete mineralization of the organism. Killing is most effective when there is close contact between the organisms and the TiO_2 catalyst. The authors also report that death efficiency can be enhanced by killing by the presence of other antimicrobials agents such as Cu and Ag.

Prasad et al. (Prasad et al., 2017) used reduced graphene oxide (rGO), which is a promising antibacterial material whose effectiveness can be improved by the addition of silver nanoparticles (nAg). In this study, the authors concluded that the mechanisms of antibacterial activity of rGO-nAg nanocomposite against several important human pathogenic bacteria are different. At the same concentration (100 μg/mL), the rGO-nAg nanocomposite was significantly more effective against all three pathogens studied than rGO or nAg. It is important to note that inhibition was much faster in the case of the nanocomposite rGO-nAg compared to nitrofurantoin (another tested antibiotic), attributed to the synergistic effects of rGO-nAg–mediated contact death. Thus, it was concluded that the synergic effect was superior to the isolated effect of each of the materials. Similarly, the mechanisms of action of silver and titanium are different, so their combined effects have made the nanomaterial more effective, with evidence of synergism (the combined effect was greater than the sum of the individual effects of the agents).

By analyzing the deviations shown in Table 7, it is possible to conclude that the higher the mean, the lower the deviation. Possibly, it is due to the nanocomposite being efficient for the 3 types of microorganisms: Gram-

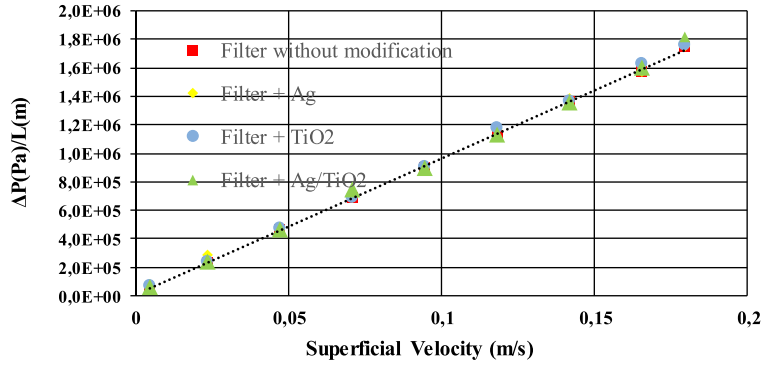

Fig. 12 $\Delta P \times L$ curve of the unmodified filter and modified filters with nanomaterials

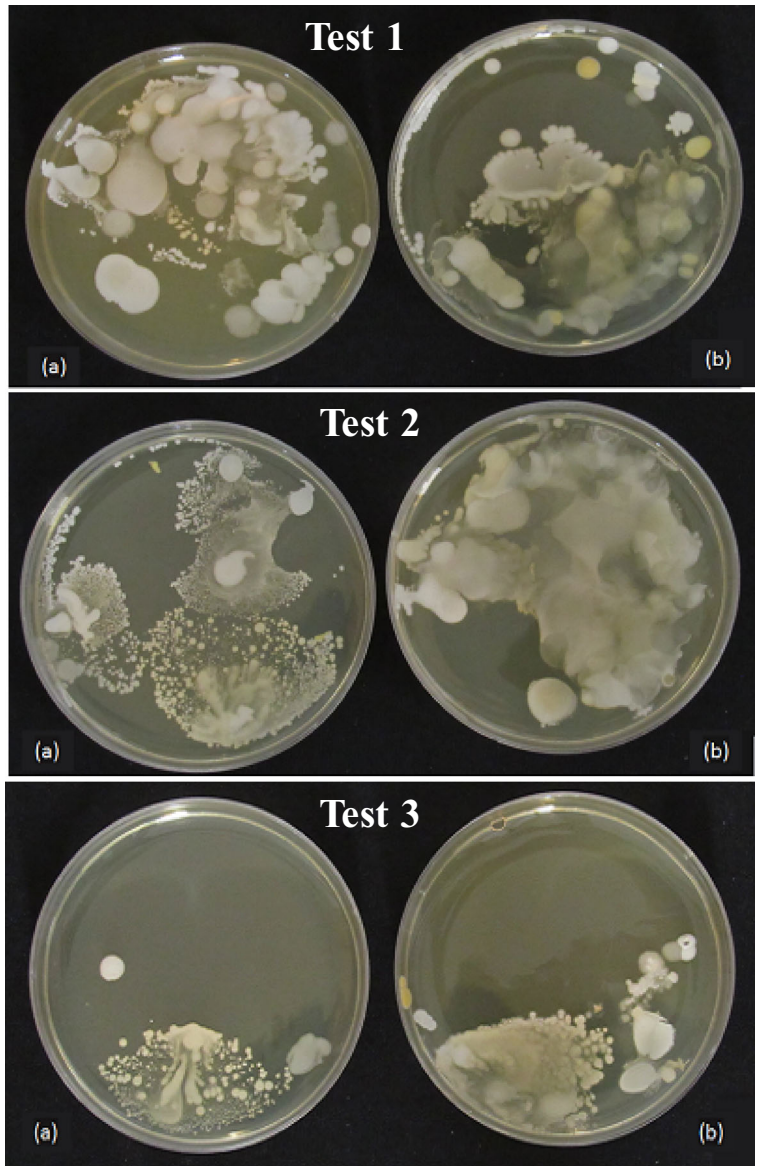

Fig. 13 Petri dishes containing the modified silver filter inoculum (**a**) and unmodified filter (**b**) incubated for 48 h. Tests 1, 2, and 3

positive bacterium, Gram-negative bacterium, and fungus. This would mean that, regardless of the variances of the population exposed to the filters, there would be good inhibition of the microorganisms and, therefore, the measurement would tend to be high and more uniform. Ag, on the other hand, is probably efficient only for one type of microorganism, which would imply that the inhibition would be low, and with greater variability, as the population exposed to the filter changed, the inhibition rate also changed.

It is important to enhance that the inhibition measured here always refers to the matter retained in the

Table 4 Dry mass and percentage of inhibition obtained in the silver tests

	Dry mass (g)	Inhibition percent (%)
Test 1		
HEPA unmodified	0.02	50.00
HEPA modified with Ag	0.04	
Test 2		
HEPA unmodified	0.02	50.00
HEPA modified with Ag	0.04	
Test 3		
HEPA unmodified	0.01	66.66
HEPA modified with Ag	0.03	

Table 5 Dry mass and percentage of inhibition obtained in the TiO_2 tests

	Dry mass (g)	Inhibition percent (%)
Test 1		
HEPA unmodified	0.06	66.66
HEPA modified with TiO_2	0.02	
Test 2		
HEPA unmodified	0.04	75.00
HEPA modified with TiO_2	0.01	
Test 3		
HEPA unmodified	0.04	75.00
HEPA modified with TiO_2	0.01	

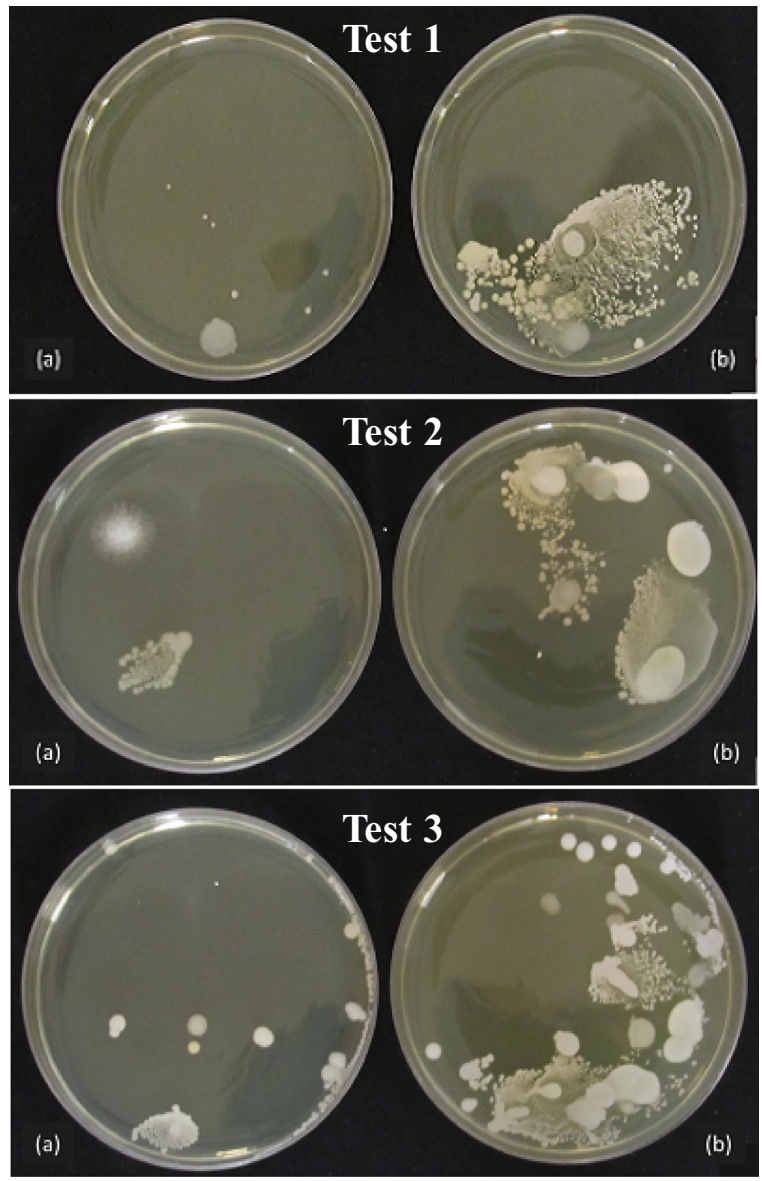

Fig. 14 Petri dishes containing the modified TiO_2 filter inoculum (**a**) and unmodified filter (**b**) incubated for 48 h. Tests 1, 2, and 3

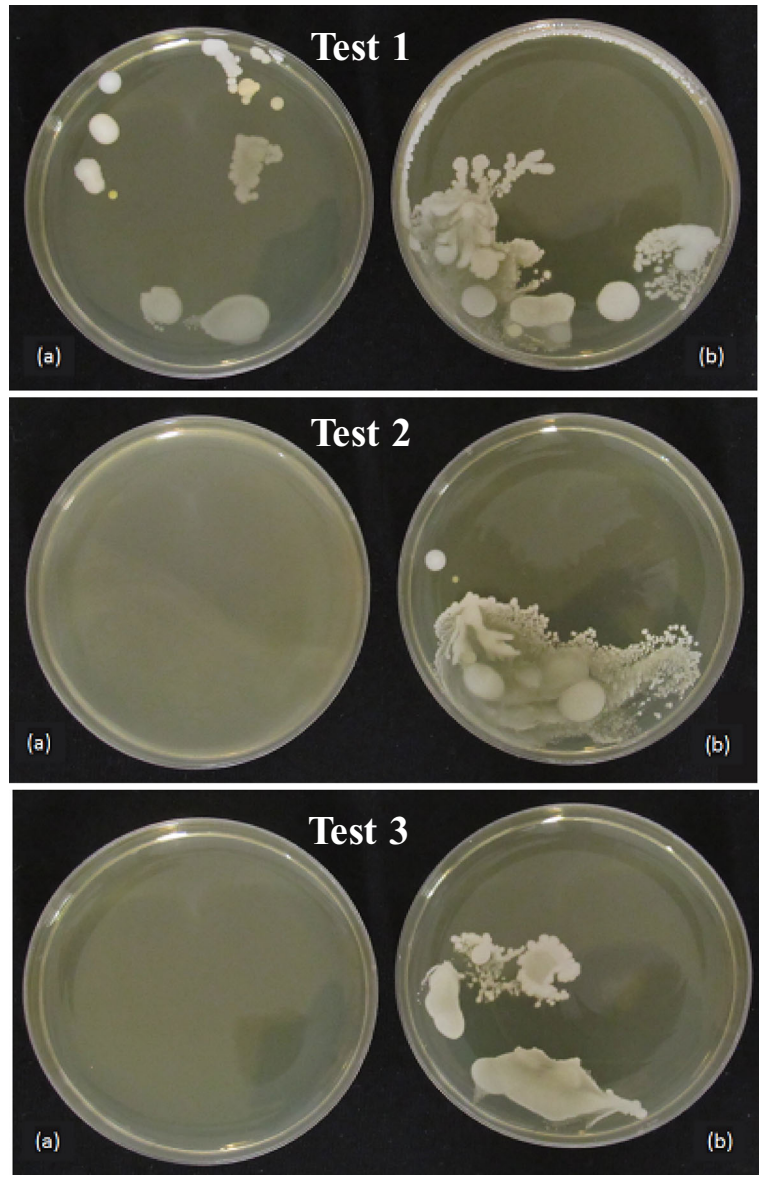

Fig. 15 Petri dishes containing the Ag/TiO_2 modified filter inoculum (**a**) and the unmodified filter (**b**) incubated for 48 h. Tests 1, 2, and 3

Table 6 Dry mass and percentage of inhibition obtained in the Ag/TiO_2 tests

	Dry mass (g)	Inhibition percent (%)
Test 1		
HEPA unmodified	0.05	80.00
HEPA modified with Ag/TiO_2	0.01	
Test 2		
HEPA unmodified	0.06	83.33
HEPA modified with Ag/TiO_2	0.01	
Test 3		
HEPA unmodified	0.05	80.00
HEPA modified with Ag/TiO_2	0.01	

Table 7 Average inhibition results obtained for the three different filters in a real environment

Nanomaterial	Mean inhibition percentage (%)
Ag	55.6 ± 9.52
TiO_2	72.2 ± 4.81
Ag/TiO_2	81.11 ± 1.92

filter since the air passing the filters has no contamination in all conditions tested. Therefore, the modification proposed in this paper probably would increase the time for using filter safely in an air-conditioner system.

4 Conclusions

This investigation aimed to evaluate the power of the elimination of microorganisms by different biocidal nanomaterials. This study indicated microorganisms' inhibitions between 53 and 75%, with the highest percentages achieved using the Ag/TiO_2 nanocomposite. These numbers suggested that the combination of the mechanisms of action of silver (damage to the cell membrane and disruption of electron transport) and titanium dioxide (photocatalytic production of reactive oxygen species that destroy microorganism cell components) was accounted for the greater effect of the hybrid material. As the mechanisms of action of silver and titanium are different, it is possible that the mixture of the two materials in the form of a composite resulted in a synergistic effect that enhanced the antimicrobial action of the nanomaterial.

This work also intended to evaluate the capability of a filter medium modified with those materials to mitigate bioaerosol contamination during a real application. The data obtained demonstrated that it is possible to minimize the concentration of bioaerosols in an internal environment using a nanoparticle-modified filter medium having an antimicrobial effect. The best elimination/inhibition rates also were to the modified filter with the Ag/TiO_2 nanocomposite (81.11 ± 1.92%), which allows us to believe that the synergistic effect also caused an improvement in the inhibition of microorganisms.

It was also possible to conclude that the addition of nanomaterials in the filter media, in the manner done in this work, did not alter its permeability. Therefore, it is not necessary to use extra energy to operate the equipment in which the filter will be disposed of.

This work showed that it is possible to minimize pollution by bioaerosols in enclosed places using surface-modified filters with aerosols of silver, titanium dioxide, and silver titania composites. These findings have significant implications for human health protection regarding respiratory diseases.

A further study could assess if similar results would be obtained for viruses (such as SARS-CoV-2). The tested materials can also be useful for the development of coatings for surfaces to inactivate microorganisms that survive on them.

Acknowledgements The authors thank the Laboratory of Pharmaceutical Processes (LAPROFAR) for the particle size analyses using the Zetasizer Nano ZS90 system (FAPESP process 2014/25934-9).

Funding This study received financial support from FAPESP (process 2014/11425-5.) and Coordination of Improvement of Higher Education Personnel (CAPES, Finance Code 001).

References

Ahmad, T., Wani, I. A., Manzoor, N., Ahmed, J., & Asiri, A. M. (2013). Biosynthesis, structural characterization and antimicrobial activity of gold and silver nanoparticles. *Colloids and Surfaces, B: Biointerfaces, 107*, 227–234.

Alizadeh, H., Salouti, M., & Shapourib, R. (2013). Intramacrophage antimicrobial effect of silver nanoparticles against Brucella melitensis 16M. *Scientia Iranica, 20*(3), 1035–1038.

Allaker, R. P. (2010). The use of nanoparticles to control oral biofilm formation. *Journal of Dental Research, 80*(11), 1175–1186.

Amooaghaie, R., Saer, R. M., & Azizi, M. (2015). Synthesis, characterization and biocompatibility of silver nanoparticles synthesized from Nigella sativa leaf extract in comparison with chemical silver nanoparticles. *Ecotoxicology and Environmental Safety, 120*, 400–408.

Arshi, N., Ahmed, F., Kumar, S., Anwar, M. S., Lu, J., Koo, B. H., & Lee, C. G. (2011). Microwave assisted synthesis of gold nanoparticles and their antibacterial activity against *Escherichia coli (E. coli)*. *Current Applied Physics, 11*, 5360–5363.

Bauer, A. W., Kirby, W. M. M., Sherris, J. C., & Turck, M. (1966). Antibiotic susceptibility testing by a standardized single disk method. *American Journal of Clinical Pathology, 45*, 493–496.

Calder, A. J., Dimkpa, C. O., Mclean, J. E., Britt, D. W., Johnson, W., & Anderson, A. J. (2012). Soil components mitigate the antimicrobial effects of silver nanoparticles towards a beneficial soil bacterium, Pseudomonas chlororaphis O6. *Science of the Total Environment, 429*, 215–222.

Cao, H., Lio, X., Meng, F., & Chu, P. K. (2011). Biological actions of silver nanoparticles embedded in titanium controlled by micro-galvanic effects. *Biomaterials, 32*, 693–705.

Catranis, C. M., et al. (2006). A new sub-sampling method for analysis of air samples collected with the Andersen single-stage sampler. *Aerobiologia, 22*, 177–184.

Combarros, R. G., Collado, S., & Díaz, M. (2016). Toxicity of titanium dioxide nanoparticles on Pseudomonas putida. *Water Research, 90*, 378–386.

Conlon, J. M., Kolodziejek, J., & Nowotny, N. (2004). Antimicrobial peptides from ranid frogs: Taxonomic and phylogenetic markers and a potential source of new therapeutic agents. *Biochimica et Biophysica Acta, 1696*, 1–14.

Costa, A. C. F., Vilar, M. A., Lira, H. L., Kiminami, R. H. G. A., & Gama, L. (2006). Síntese e caracterização de nanopartículas de TiO2. *Cerâmica, 52*(324), 255–259.

Durairaj, B., Xavier, T., & Muthu, S. (2014). Fungal generated titanium dioxide nanoparticles for UV protective and bacterial resistant fabrication. *International Journal of Engineering, Science and Technology, 6*(9), 621–625.

Estruga, M., Domingo, C., & Ayllón, J. A. (2010). Microwave radiation as heating method in the synthesis of titanium dioxide nanoparticles from hexafluorotitanate-organic salts. *Materials Research Bulletin, 45*, 1224–1229.

Eustis Krylova, G., Eremenko, A., Smirnova, N., Schilla, A. W., & El-Sayed, M. (2005). Growth and fragmentation of silver nanoparticles in their synthesis with a fs laser and CW light by photo-sensitization with benzophenone. *Photochemical & Photobiological Sciences, 4*, 154–159.

Ferreira, V. S., Ferreira, M. E. C., Lima, L. M. T. R., Frasés, S., Souza, W., & Sant'Anna, C. (2017). Green production of microalgae-based silver chloride nanoparticles with antimicrobial activity against pathogenic bacteria. *Enzyme and Microbial Technology - Journal, 97*, 114–121.

Filpo, G., Palermo, A., Rachiele, F., & Nicoletta, F. P. (2013). Preventing fungal growth in wood by titanium dioxide nanoparticles. *International Biodeterioration & Biodegradation, 83*, 217–222.

Foster, H. A., et al. (2011). Photocatalytic disinfection using titanium dioxide: Spectrum and mechanism of antimicrobial activity. *Applied Microbiology and Biotechnology, 90*, 1847–1868.

Freitas, A. R., Baeza, L. C., Faria, M. G. I., Dota, K. F. D., Martínez, P. G., & Svidzinski, T. I. R. (2014). Yeasts isolated from nosocomial urinary infections: Antifungal susceptibility and biofilm production. *Revista Iberoamericana de Micología, 31*(2), 104–108.

Gorup, L. F., Longo, E., Leite, E. R., & Camargo, E. R. (2011). Moderating effect of ammonia on particle growth and stability of quasi-monodisperse silver nanoparticles synthesized by the Turkevich method. *Journal of Colloid and Interface Science, 360*, 355–358.

Hassanjani-Roshana, A., Kazemzadeha, S. M., Vaezia, M. R., & Shokuhfarc, A. (2011). The effect of sonication power on the sonochemical synthesis of titania nanoparticles. *Journal of Ceramic Processing, 12*(3), 299–303.

Hebeish, A., Hashem, M., Abd El-Hady, M. M., & Sharaf, S. (2013). Development of CMC hydrogels loaded with silver nano-particles for medical applications. *Carbohydrate Polymers, 92*, 407–413.

Kim, Y. J., Platt, U., Gu, M. B., & Iwahashi, H. (2009). *Atmospheric and biological environmental monitoring*. Springer.

Krutyakov, Y. A., Olenin, A. Y., Kudrinskii, A. A., Dzhurik, P. S., & Lisichkin, G. V. (2008). Aggregative stability and polydispersity of silver nanoparticles prepared using two-p aqueous organic systems. *Nanotechnologies in Russia, 3*(5-6), 303–310.

Kumar, B., Smita, K., Cumbal, L., & Debut, A. (2017). Green synthesis of silver nanoparticles using Andean blackberry fruit extract. *Saudi Journal of Biological Sciences, 24*(1), 45–50.

Lazarevic, Z. Z., Vijatovic, M., Dohcevic-Mitrovic, C., Romcevic, N. Z., Romcevic, M. J., Paunovic, N., & Stojanovic, B. D. (2010). The characterization of the barium titanate ceramic powders prepared by the Pechini type reaction route and mechanically assisted synthesis. *Journal of the European Ceramic Society, 30*, 623–628.

Le Ouay, B., & Stellacci, F. (2015). Antibacterial activity of silver nanoparticles: A surface science insight. *Nano Today, 10*(3), 339–354. https://doi.org/10.1016/j.nantod.2015.04.002.

Lee, P. C., & Meisel, D. (1982). Adsorption and surface-enhanced Raman of dyes on silver and gold sols. *The Journal of Physical Chemistry, 86*, 3391.

Ma, H., Yin, B., Wang, S., Jiao, Y., Pan, W., Huang, S., Chen, S., & Meng, F. (2004). Synthesis of silver and gold nanoparticles by a novel electrochemical method. *Chemphyschem, 5*, 68–75.

Malekfar, R., Ahmadi, G., Cheraghi, A., Rohollahnejad, J., Sahraiyan, F., & Khanzadeh, M. (2009). Micro-Raman scattering of KTP (KTiOPO4) nanocrystallites synthesized by modified sol–gel Pechini method. *Vibrational Spectroscopy, 51*, 308–312.

Ninan, N., Muthiah, M., Bt Yahaya, N. A., Park, I., Elain, A., Wong, T. W., Thomas, S., & Grohens, Y. (2014). Antibacterial and wound healing analysis of gelatin/zeolite scaffolds. *Colloids and Surfaces, B: Biointerfaces, 115*, 244–252.

Nurul Aini, A., Al Farraj, D. A., Endarko, E., et al. (2019). A new green method for the synthesis of silver nanoparticles and their antibacterial activities against gram-positive and gram negative bacteria. *Journal of the Chinese Chemical Society, 64*, 1–8.

Palanisamy, S., Rajasekar, P., Vijayaprasath, G., Ravi, G., Manikandan, R., & Prabhu, N. M. (2017). A green route to synthesis silver nanoparticles using Sargassum polycystum and its antioxidant and cytotoxic effects: An in vitro analysis. *Materials Letters, 185*, 196–200.

Pan, X., et al. (2010). Nanocharacterization and bactericidal performance of silver modified titania photocatalyst. *Colloids and Surfaces, B: Biointerfaces, 77*, 82–89.

Panacek, A., Kolar, M., Vecerova, R., Prucek, R., Soukupova, J., Krystof, V., Hamal, P., Zboril, R., & Kvitek, L. (2009). Antifungal activity of silver nanoparticles against *Candida spp*. *Biomaterials, 30*, 6333–6340.

Pechini, M. P. (1967). Method of preparing lead and alkaline earth titanates and niobates and coating method using the same to form a capacitor. United States Patent Office. U.S. Patent 3.330.697, July 11, 1967.

Pillai, Z. S., & Kamat, P. V. (2004). What factors control the size and shape of silver nanoparticles in the citrate ion reduction

method? *The Journal of Physical Chemistry. B, 108*, 945–951.

Prasad, K., et al. (2017). Synergic bactericidal effects of reduced graphene oxide and silver nanoparticles against Gram-positive and Gram-negative bacteria. *Nature Scientific Reports, 7*(1591), 1–11.

Prema, P., Thangapandiyanb, S., & Immanuel, G. (2017). CMC stabilized nano silver synthesis, characterization and its antibacterial and synergistic effect with broad spectrum antibiotics. *Carbohydrate Polymers, 158*, 141–148.

Raja, S., Ramesh, V., & Thivaharan, V. (2017). Green biosynthesis of silver nanoparticles using Calliandra haematocephala leaf extract, their antibacterial activity and hydrogen peroxide sensing capability. *Arabian Journal of Chemistry, 10*, 253–261.

Rajagopal, G., et al. (2006). Biocidal effects of photocatalytic semiconductor TiO2. *Colloids and Surfaces B: Biointerfaces, 51*, 107–111.

Ravichandran, K., Nithiyadevi, K., Sakthivel, B., Arun, T., Sindhuja, E., & Muruganandam, G. (2016). Synthesis of ZnO:Co/rGO nanocomposites for enhanced photocatalytic and antibacterial activities. *Ceramics International, 42*, 17539–17550.

Rosa, P. F., et al. (2017). Modification of cotton fabrics with silver nanoparticles for use in conditioner air to minimize the bioaerosol concentration in indoor environments. *Water, Air, and Soil Pollution, 228*, 244.

Rosa, P. F., Martins, J. C., Lima, B. A., Oishi, M., Aguiar, M. L., & Bernardo, A. (2018). Atomization of silver nanoparticles suspension as an alternative for generating nanosilver aerosol. *Chemical Industry and Chemical Engineering Quarterly, 24*(4), 303–307.

Ross, M. A., Curtis, L., Scheff, P. A., Hryhorczuk, D. O., Ramakrishnan, V., Wadden, R. A., & Persky, V. W. (2000). Association of asthma symptoms and severity with indoor bioaerosols. *Allergy, 55*, 705–711.

Šalkus, T., Barre, M., Kežionis, A., Kazakevičius, E., Bohnke, O., Selskienė, A., & Orliukas, A. F. (2012). Ionic conductivity of Li1.3Al0.3−xScxTi1.7(PO4)3 (x = 0, 0.1, 0.15, 0.2, 0.3) solid electrolytes prepared by Pechini process. *Solid State Ionics, 225*, 615–619.

Selvamani, M., Krishnamoorthy, G., Ramadoss, M., Sivakumar, P. K., Settu, M., Ranganathan, S., & Vengidusamy, N. (2016). Ag@Ag8W4O16 nanoroasted rice beads with photocatalytic, antibacterial and anticancer activity. *Materials Science and Engineering: C, 60*, 109–118.

Sivaranjani, V., & Philominathan, P. (2016). Synthesize of titanium dioxide nanoparticles using Moringa oleifera leaves and evaluation of wound healing activity. *Wound Medicine, 12*, 1–5.

Suman, T. Y., Ravindranath, R. R. S., Elumalai, D., Kaleena, P. K., Ramkumar, R., Perumal, P., Aranganathan, L., & Chitrarasu, P. S. (2015). Larvicidal activity of titanium dioxide nanoparticles synthesized using Morinda citrifolia root extract against Anopheles stephensi, Aedes aegypti and Culex quinquefasciatus and its other effect on non-target fish. *Asian Pacific Journal of Tropical Disease, 5*(3), 224–230.

Syafiuddin, A., Salmiati, Hadibarata, T., et al. (2017). A purely green synthesis of silver nanoparticles using Carica papaya, Manihot esculenta, and Morinda citrifolia: Synthesis and antibacterial evaluations. *Bioprocess and Biosystems Engineering, 40*, 1349–1361.

Syafiuddin, A., et al. (2018). Novel weed-extracted silver nanoparticles and their antibacterial appraisal against a rare bacterium from river and sewage treatment plan. *Nanomaterials (Basel), 8*(9), 1–17.

Tian, J., Tu, H., Shi, X., Wang, X., Deng, H., Li, B., & Du, Y. (2016). Antimicrobial application of nanofibrous mats self-assembled with chitosan and epigallocatechin gallate. *Colloids and Surfaces, B: Biointerfaces, 145*, 643–652.

Tortora, G.J.; Funke, B.R.; Case, C.L. Microbiologia. Artmed, 8a edição, 2006.

Turkevich, J., Stevenson, P. C., & Hillier. (1951). A study of the nucleation and growth processes in the synthesis of colloidal gold. *Journal Discussions of the Faraday Society, 11*, 55–75.

Turki, Y., Ouzari, H., Mehri, I., Ammar, A. B., & Hassen, A. (2012). Evaluation of a cocktail of three bacteriophages for the biocontrol of Salmonella of wastewater. *Food Research International, 45*, 1099–1105.

WHO. (2017). World Health Association, Accessed on 03/01/2017. http://www.who.int/mediacentre/news/releases/2016/air-pollution-rising/en/.

Xia, Z., Ma, Q., Li, S., Zhang, D., Cong, L., Tian, Y., & Yang, R. (2016). The antifungal effect of silver nanoparticles on Trichosporon asahii. *Journal of Microbiology, Immunology, 49*, 182–188.

Zhang, W., Qiao, X., & Chen, J. (2007). Synthesis of nanosilver colloidal particles in water/oil microemulsion. *Colloids and Surfaces A: Physicochemical and Engineering Aspects, 299*, 22–28.